Fuel 364 (2024) 130788

Contents lists available at ScienceDirect

Fuel

journal homepage: www.elsevier.com/locate/fuel

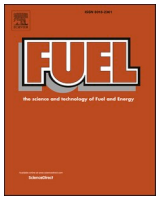

Full Length Article

Bed material performance of quartz, natural K-feldspar, and olivine in bubbling fluidized bed combustion of barley straw

Marjan Bozaghian Bäckman [a,b,*], Anders Rebbling [a], Matthias Kuba [c,d], Sylvia H. Larsson [b], Nils Skoglund [a,e]

[a] Thermochemical Energy Conversion Laboratory, Department of Applied Physics and Electronics, Umeå University, SE-901 87 Umeå, Sweden
[b] Department of Forest Biomaterials and Technology, Swedish University of Agricultural Sciences, SE-901 83 Umeå, Sweden
[c] BEST Bioenergy and Sustainable Technologies GmbH, Graz 8010, Austria
[d] Institute of Chemical, Environmental and Bioscience Engineering, TU Wien, Vienna 1060, Austria
[e] Energy Engineering, Division of Energy Science, Luleå University of Technology, SE-971 87 Luleå, Sweden

ARTICLE INFO

Keywords:
Agricultural residue
Agglomeration
Bed particle
Layer formation
Bioenergy

ABSTRACT

The present study investigates how three different silicate-based bed materials behave in bubbling fluidized bed combustion of a model agricultural residue with respect to ash composition, namely barley straw. Quartz, natural K-feldspar, and olivine were all used in combustion at 700 °C, and the resulting layer formation and bed agglomeration characteristics were determined. Based on this, a general reaction model for bed ash from agricultural residues was proposed, taking into account the reactivity of the different silicates investigated towards the main ash-forming elements K, Ca, and Si. The proposed reaction model links bed material interaction with K-rich bed ash to the degree of polymerization of the silicate bed material, where addition reactions occur in systems with high polymerization, predominately in quartz, and substitution reactions dominate for depolymerized silicates such as K-feldspar and olivine.

1. Introduction

The share of bioenergy in the global net energy supply should increase to meet recommendations from IPCC [1] and the Net Zero Emission by 2050 goals set by IEA [2]. For this increase in bioenergy to align with the sustainable development goals defined by the United Nations [3], residual streams from forestry and agriculture will be expected to become increasingly important fuel feedstocks. A successful implementation of such residues in the bioenergy sector depends on whether they can be used safely and predictably in available conversion technologies such as powder combustion, fixed beds, or fluidized beds – the latter of which is the topic of the present work.

While conversion of the energy-carrying carbonaceous matrix in biomass generally works well in these technologies, the overall ash composition and ash transformation reactions have been shown to pose a larger challenge [3,4]. A challenge specific to thermochemical conversion fluidized beds is the interaction between the ash-forming elements and the bed material, where different biomass types may result in different interaction types [5-11]. Quartz is commonly used as bed material in fluidized beds, but alternatives such as olivine [5,12-14] or feldspars [15-18] are of increasing interest due to different interaction pathways with bed ash.

The general mechanism of converting woody-type biomass in fluidized beds is generally well described in the literature for several types of bed materials [5-7,10,13,19]. The generally low ash melting temperature from agricultural residues, including different pathways to layer formation with different bed materials, is a continued challenge [20,21]. The reaction pathways are of particular interest when determining a suitable bed material for fluidized bed conversion of agricultural residues, where the bed performance is further influenced by the often low-temperature melting ash.

Altering the chemical composition of fuel intended for combustion by incorporating materials that lack heating value, also known as additivation, is a well-researched approach to mitigate ash-related issues during fluidized bed combustion [22-26] and other common biomass combustion technologies [27-31]. In a study by Bozaghian et al., [32], the combustion characteristics of barley straw pre-treated and stored with $CaCO_3$ as a measure for reducing ash-related problems

* Corresponding author at: Thermochemical Energy Conversion Laboratory, Department of Apllied Physics and Electronics, Umeå University, SE-901 87 Umeå, Sweden.
E-mail address: marjan.bozaghian@umu.se (M. Bozaghian Bäckman).

https://doi.org/10.1016/j.fuel.2023.130788
Received 20 October 2023; Received in revised form 21 December 2023; Accepted 27 December 2023

Table 1
Fuel analysis with moisture content, ash content, and elemental composition with main ash forming elements. The same barley straw was previously studied with $CaCO_3$ additivation by Bozaghian et al. [32].

Fuel properties		
Moisture content	wt-%	9.8
Ash	wt-% d.b.	4.7
C	wt-% d.b.	47.3
H	wt-% d.b.	5.6
N	wt-% d.b.	0.46
O	wt-% d.b.	41.6
K	mg/kg d.b.	11,000
Na	mg/kg d.b.	74
Ca	mg/kg d.b.	5000
Mg	mg/kg d.b.	670
Fe	mg/kg d.b.	75
Al	mg/kg d.b.	39
Si	mg/kg d.b.	5100
P	mg/kg d.b.	410
S	mg/kg d.b.	740
Cl	mg/kg d.b.	1550

d.b. = dry basis.

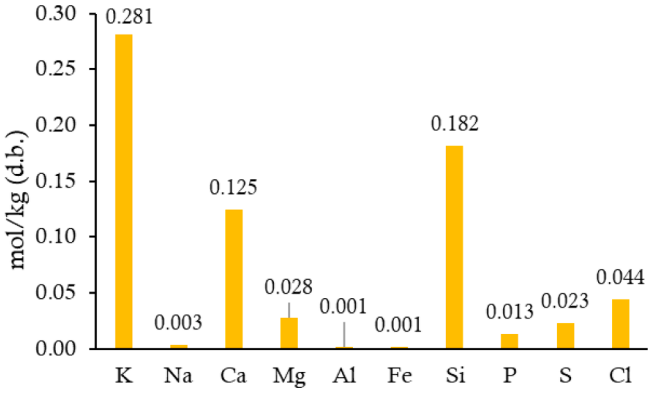

Fig. 1. Fuel fingerprint for easy comparison of main ash-forming element concentrations. The dominant ash-forming elements in barley straw are K-Si-Ca, typical for many agricultural residues.

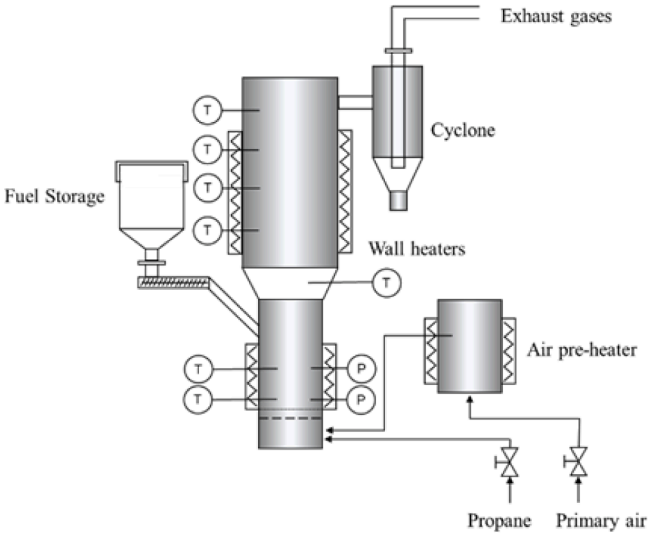

Fig. 2. Schematic view of the bubbling fluidized bed used for combustion and agglomeration experiments. Positions for upper and lower bed temperatures, as well as upper and lower bed pressure, are indicated in the bottom left above the air distribution plate represented by a dashed line.

Table 2
Initial and total defluidization temperature (d.t.) for the respective bed materials as defined in Figs. 4, 6, and 8 for each bed material.

	Quartz	Feldspar	Olivine
Initial d.t. (°C)	780	720	815
Total d.t. (°C)	850	735	830

were empirically evaluated in a bubbling fluidized bed combustion. The study showed that the use of Ca-additives to mitigate alkali-induced ash-related problems is a balancing act between retaining alkali in silicates with higher melting temperatures or releasing it into the flue gas as particulate matter or volatile species [32]. Therefore, finding alternative bed materials to the commonly used quartz is of interest in cases where additivation is not desired or possible.

In fluidized bed combustion using quartz, the dominating mechanism for interaction between bed ash and bed material particles is linked to the formation of layers on the bed material consisting of K-silicates and Ca-K-silicates. The mechanism is well described in the literature [10,11,33] and can be summarized as follows: an initial attack of K-compounds such as KOH(g) reacts with the surface of the quartz particle to form an inner layer of K-silicate. This layer has a low melting temperature and may, therefore, lead to the formation of agglomerates via physical adhesion of the layer with bed material or ash particles. If the chemical composition of the bed ash is as such, a substitution reaction can occur where Ca reacts into the bed particle, typically forming an outer layer of adhering bed ash. Such Ca-K-silicates generally have a higher melting temperature compared to K-silicates, and from a bed agglomeration point of view is more beneficial. In this respect, quartz can be considered to be quite reactive toward bed ash as it may react in several steps.

The mechanisms of bed layer formation on olivine have been described as a solid–solid substitution reaction forming Ca-rich coatings on the bed particles [7]. Another possible route may be the ionic transport of Ca^{2+}, resulting in the formation of intermediary Ca-Mg-silicates and a subsequent complete substitution of Mg [34,35]. This could lead to the formation of cracks in the bed material, thus increasing the area available for further reactions.

Feldspars have slightly different tendencies for reaction depending on what type it is, although the general reaction pathway could be described as a substitution reaction similar to that of olivine with features from quartz. Na-feldspars may react with K-compounds where Na^+ is substituted by K^+ to form K-feldspar [17]. Both types react with Ca^{2+} by substitution reactions to form Ca-aluminosilicates, displacing alkali from bed particles out to the bed ash [5,15-18,36].

The present work aims to compare the performance of three different silicate-based bed materials, quartz; natural K-feldspar; and olivine, in bubbling fluidized bed combustion of the agricultural residue barley straw. The resulting bed ash interaction with these materials for bed agglomeration temperature is determined and the responsible mechanisms discussed, including the wider implications for bed material selection in bubbling fluidized bed conversion of agricultural residues.

2. Material and method

2.1. Fuel and bed materials

Barley straw harvested in northern Sweden was selected as a typical K-Si-rich biomass fuel from agricultural residues. Standard fuel analyses were performed according to standards for ash content (SS-EN 14775:2009), sulphur (SS-EN ISO 16,994:2015), and chlorine (SS-EN ISO 16994:2015). Volatile elemental composition (C, H, N) were determined according to SS-EN ISO 16948:2015 with oxygen (O) calculated according to standard SS-EN 14918:2010. Main ash-forming elements were determined according to standard SS-EN 15290:2011 with inductively coupled plasma—atomic emission spectroscopy (ICP-

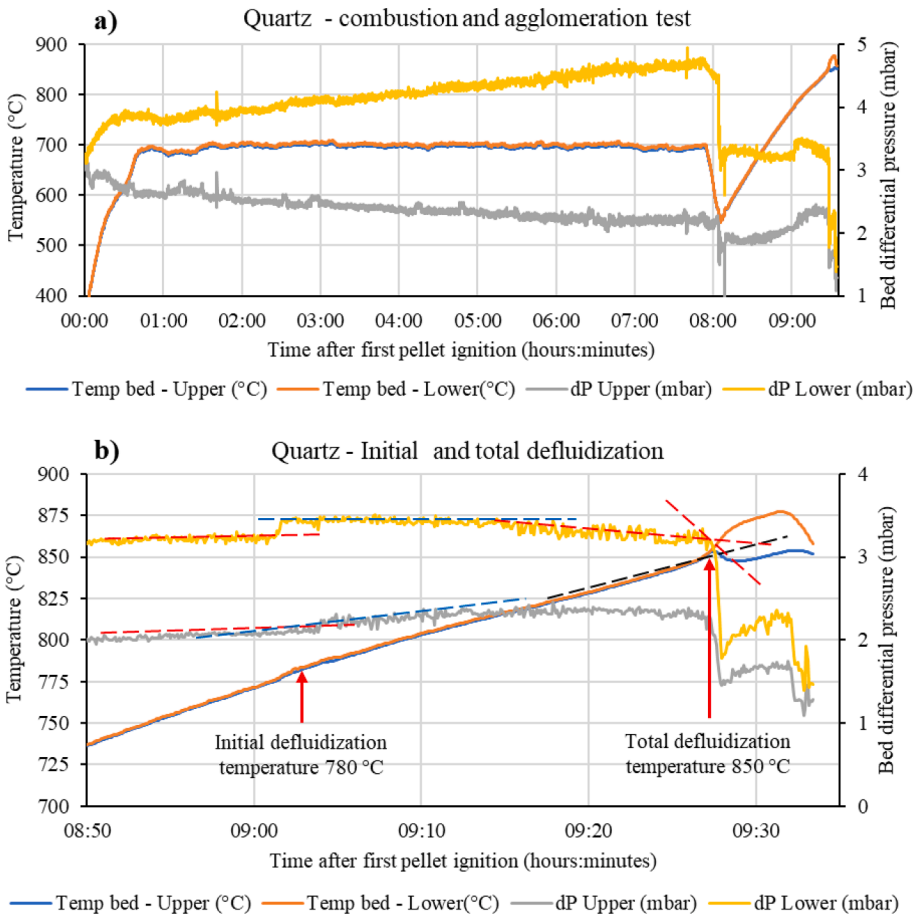

Fig. 3. Barley straw combustion in bubbling fluidized bed using quartz as bed material a) bed material characteristics in terms of bed temperature and differential pressure trends, including agglomeration test after 8 h of operation, b) Identification of initial and total defluidization temperature. Lines supporting the conclusions are indicated in the figure; initial defluidization temperature occurred at ~ 780 °C based on changes in bed pressures and a slight deviation in bed temperature. Total defluidization temperature was identified at ~ 850 °C based on the initiated major temperature change and sharp drops in bed pressures just prior to the complete agglomeration of the bed.

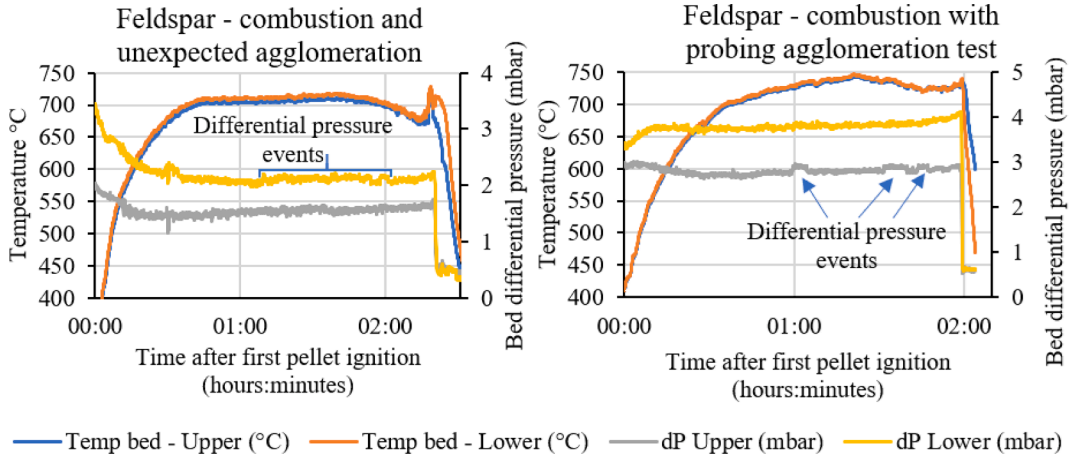

Fig. 4. Bed material characteristics in bubbling fluidized bed combustion of barley straw using feldspar as bed material in terms of bed temperature and differential pressure trends. Left figure displays the intended 700 °C operation mode, including unexpected agglomeration. The right figure displays the outcome when the bed was operated at a higher temperature to identify probable initial and total defluidization temperatures. The instability of the bed is visible as differential pressure events throughout the short 2-hour operation period in both cases.

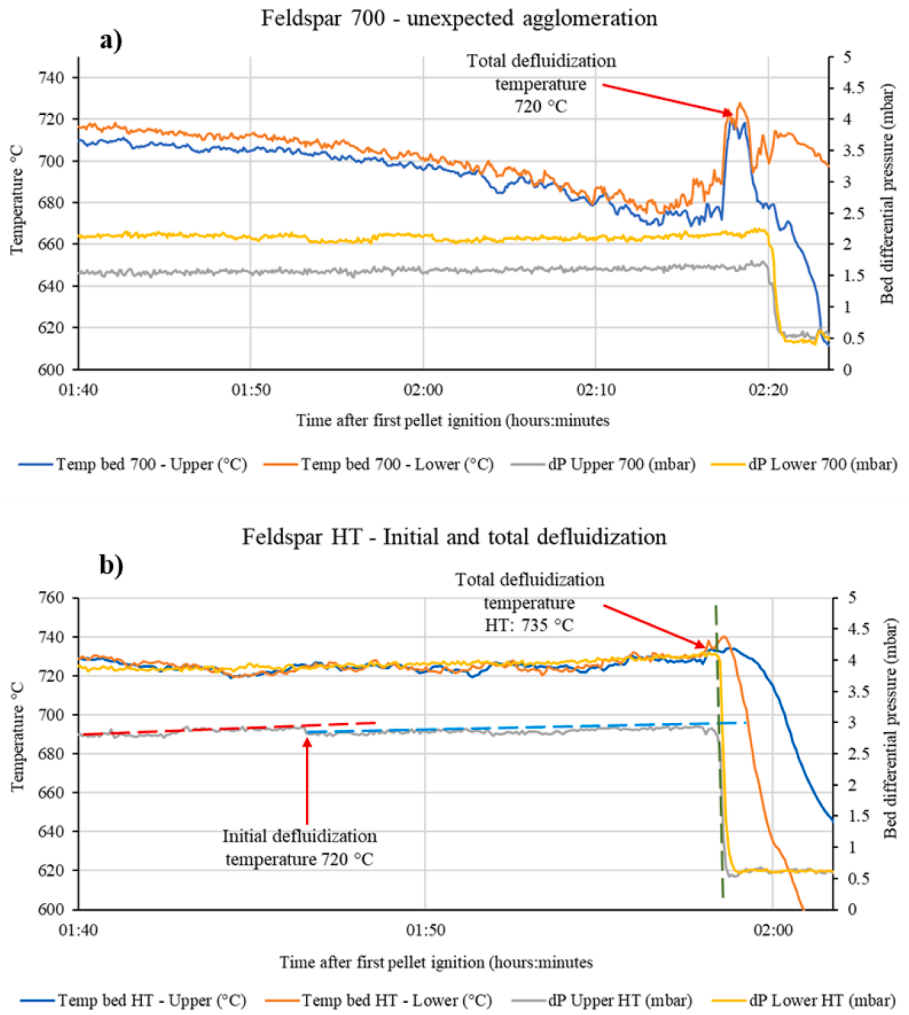

Fig. 5. Identification of initial and total defluidization temperature in bubbling fluidized bed combustion of barley straw using feldspar as bed material based on a) experiment at 700 °C (labeled 700) or b) elevated bed temperature (labeled HT). Lines supporting the conclusions are indicated in the figure b); initial defluidization temperature occurred at ~ 720 °C based on changes in bed pressures and a slight deviation in bed temperature in the HT experiment. Total defluidization temperature was identified at ~ 735 °C for the HT case based on the initiated temperature change and sharp drops in bed pressures. This was notably higher than the 720 °C observed in the experiment with 700 °C bed temperature, figure a.

AES). The elemental fuel analysis with main ash-forming elements is presented in Table 1 and Fig. 1.

The bed materials were chosen to represent commercially available products with significantly different chemical structure and composition. Quartz (SiO_2) is a tectosilicate consisting of linked Si-O tetrahedra, and the purity of the material used in this study was determined by powder X-ray diffraction (XRD) to be above 98 %. Feldspar is a monoclinic tectosilicate mineral, and the XRD analysis indicated that the composition in the natural feldspar used here was 58 % K- and Na-feldspar with 42 % quartz inclusion. Olivine is an orthorhombic neosilicate with a composition that can vary between Mg_2SiO_4 and Fe_2SiO_4. The olivine used was analyzed by XRD and found to consist of 90 % Mg_2SiO_4 with some inclusion of quartz.

2.2. Combustion experiments

Combustion experiments were performed in a 2-meter high 5 kW_{th} bench-scale bubbling fluidized bed shown in Fig. 2. For each experiment, 540 g of the three respective bed materials were sieved to a diameter of 200 μm < d < 250 μm using standard test sieves (ISO 3310). The pelletized barley straw was sieved to remove fine fuel particles and homogenize with respect to pellet size. Approximately 4 kg of prepared fuel was combusted with a target temperature of ~ 700 °C for 8 h or until defluidization occurred. This low temperature was selected due to the challenges with K-silicate melt formation of the fuel ash composition (Fig. 1). Each experiment started at a low temperature to, if possible, avoid bed agglomeration.

If defluidization did not occur within 8 h of combustion, the fuel feeding was stopped, and a bed sample was extracted via cyclone to attain a representative bed sample for normal operation (pre-agglomeration for quartz and olivine). K-feldspar experiments were run twice; one where early agglomeration was attained. After this, a controlled agglomeration test was initiated in accordance with the method previously described by Öhman and Nordin [37]. The total defluidization temperature is determined by gradually heating the bed and has been shown to be accurate to within ± 5 °C [37]. The resulting agglomerated bed samples were collected after the fluidized bed had cooled down sufficiently. Initial and total defluidization temperatures were determined by upper and lower bed temperature and pressure. A linear regression analysis was performed on the process data to ascertain the derivative over 10 data points, aiming to validate the initial and total defluidization temperatures for each fuel (see supplementary S1). The resulting plots of the derivatives contained both variations caused by the electrical heaters and process changes induced by the interactions between bed and ash particles (see supplementary S1). The initial defluidization temperature was determined as the first deviation in the

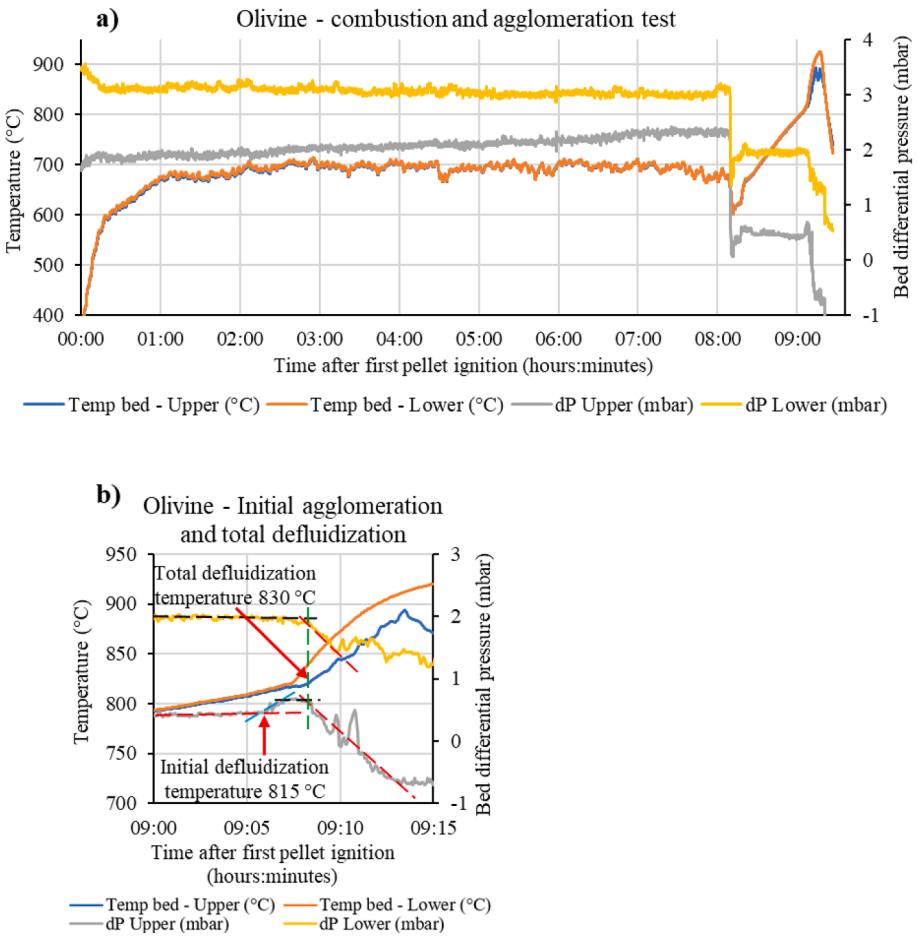

Fig. 6. Barley straw combustion in bubbling fluidized bed using olivine as bed material a) bed material characteristics in terms of bed temperature and differential pressure trends, including agglomeration test after 8 h of operation, b) Identification of initial and total defluidization temperature. Lines supporting the conclusions are indicated in the figure; initial defluidization temperature occurred at ~ 815 °C based on changes in bed pressures and a slight deviation in bed temperature. Total defluidization temperature was identified at ~ 830 °C based on the initiated major temperature difference between upper and lower bed temperature accompanied by simultaneous in bed differential pressures.

1st derivative from baseline, in either bed temperature or bed pressure.

2.3. Bed material analysis

Collected bed samples from before (quartz and olivine) and after (quartz, K-feldspar, and olivine) agglomeration were sieved (Ø = 200 μm) to separate bed ash particles and agglomerates from bed material. The agglomerates from quartz and olivine were further separated from bed ash particles post-agglomeration using a sieve (Ø = 250 μm). A sub-volume of each material type was molded in epoxy resin and polished to achieve a smooth, flat surface with cross-section of bed particles, bed ash particles, and agglomerates prior to analysis with scanning electron microscopy coupled with energy dispersive X-ray spectroscopy (SEM-EDS). The instrument used was a Carl Zeiss EVO-LS15 equipped with an Oxford X-Max EDS detector available through the Umeå Core Facility for Electron Microscopy, Umeå University. The acceleration current used was 20 kV. Each ned sample was scanned and analyzed by SEM-mapping to identify typical distributions of bed material, bed ash, and interaction layers for each bed material.

A combination of spot-, line-, and area analysis on representative areas identified by EDS mapping were used to analyze the samples morphology and chemical composition. The bed material and ash particles were classified according to outer layer, inner layer, agglomerate necks, or bed ash.

3. Results

3.1. Bed material performance

Barley straw combustion with K-feldspar as bed material caused early total defluidization, where a performance decrease was observed already after reaching 710 °C, which occurred after approximately an hour of fuel feed and uneven process performance. Therefore, this test was repeated with a stepped ramping of conversion temperature in an attempt to more clearly identify initial and total defluidization temperatures. Quartz and olivine bed materials enabled combustion for the full 8 h planned. The resulting initial and total defluidization temperatures, as identified from bed temperatures and pressures, are summarized in Table 2.

Barley straw combustion with quartz as bed material displays a common behavior with stable temperature curves (Fig. 3a). It should be noted that the lower bed pressure increases significantly over time, which may be related to some bed material adhesion in addition to the increased bed mass due to ash addition. The initial (780 °C) and total (850 °C) defluidization temperatures were identified based on bed temperatures and differential pressures, as shown in Fig. 3b.

The bed behavior of a natural K-feldspar together with barley straw bed ash displayed swings in bed differential pressure already at the intended normal operation of 700 °C, see Fig. 4. This also led to temperature swings before unexpected agglomeration occurred just over two hours after the first pellet ignited without a clearly identifiable

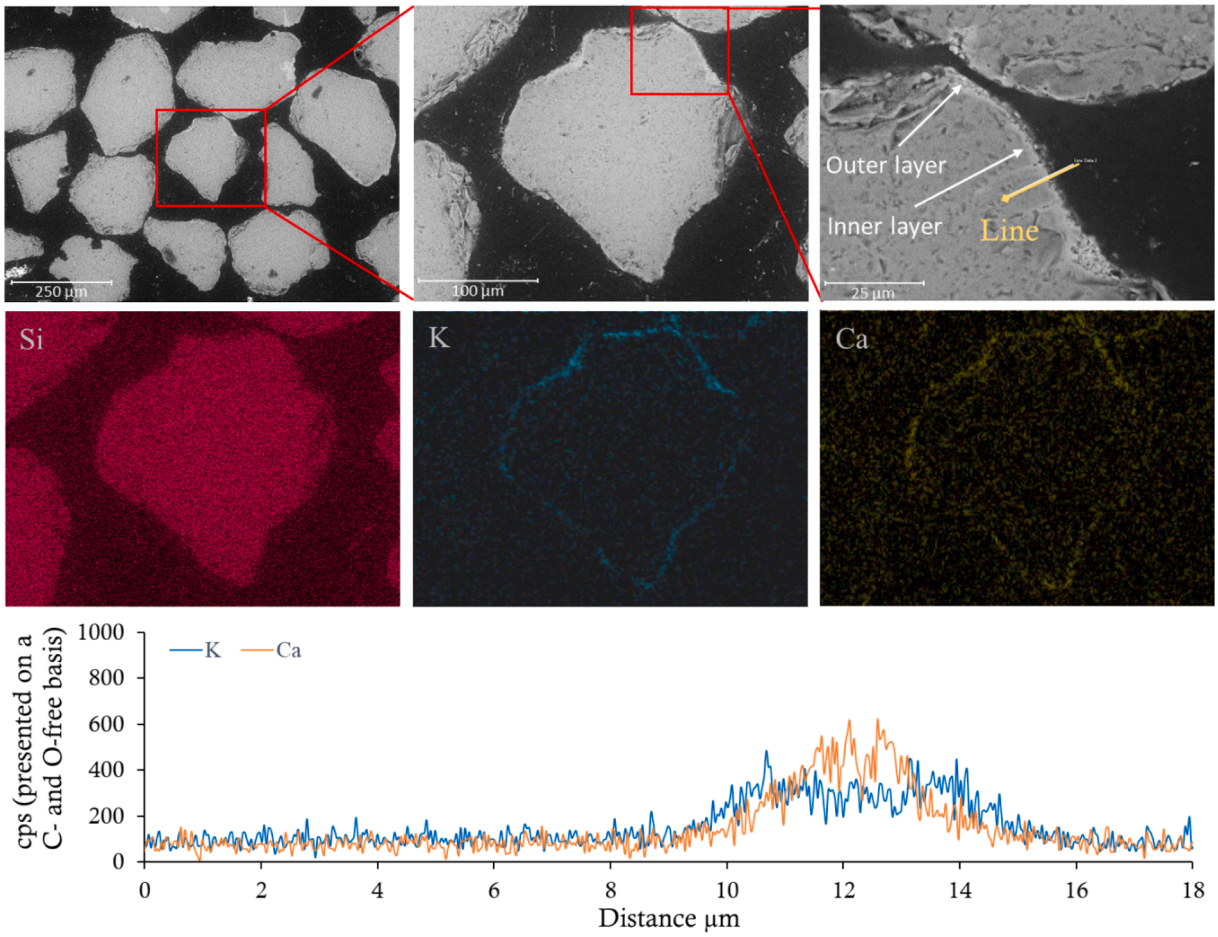

Fig. 7. BSE-SEM micrograph of a typical quartz bed particle after 8 h of barley straw combustion. Layers formed due to interaction with bed material are labeled as inner layer or outer layer in accordance with literature. The EDS line analysis shows a Ca-rich intermediate outer layer, whereas K-silicates are slightly higher in concentration closer to the particle core.

temperature for initial defluidization. Therefore, the second K-feldspar experiment aimed at providing a sufficiently stable bed temperature to identify the initial and total defluidization temperature. The second experiment provided a more stable operation; the initial (~720 °C) and total (~735 °C) defluidization temperatures could be determined (see Fig. 5a and b).

Olivine displayed stable bed differential pressures as bed material in combustion of barley straw (see Fig. 6a). The initial (815 °C) and total defluidization temperatures occurred close in temperature, where the actual temperature split between upper and lower bed temperature was observed only 5 °C above the initial defluidization temperature. Based on the bed pressure, the total defluidization was estimated at an average between upper and lower bed temperature of 830 °C (see Fig. 6b).

3.2. Layer formation

Quartz particles developed a continuous inner layer as a result of their reaction with potassium-rich compounds from the barley straw bed ash. However, the outer layers observed on the quartz particles could be found as either continuous or non-continuous layers. Reaction in inner layers Ca was observed in bed samples before agglomeration tests (Fig. 7) and after agglomeration (Fig. 8). Total layer thicknesses were commonly in the range of 3–5 µm. The natural K-feldspar displayed a more complex interaction pattern between bed ash and bed particles despite the very brief reaction time of ~ 2 h. The K-feldspar particles were either nearly unreacted (Fig. 9) or displayed thin layers of reaction with Ca (Fig. 10). Na-feldspars, present both as inclusions in K-feldspar but also as separate particles, may have reacted both with K-compounds from the bed ash but also with Ca. The quartz particles in natural feldspar had layers of similar thickness as observed in quartz after 8 h of combustion, with reactions with K-compounds being the dominant reaction pathway.

Layer formation on olivine bed particles was dominated by non-continuous outer layers rich in K (Fig. 11). Some minor interaction with inner layer formation could be observed in the bed sample collected after bed agglomeration test, see Fig. 12. The olivine bed particles showed the lowest degree of interaction with the barley straw bed ash of the bed materials investigated in the present work. This makes the melting point of the bed ash itself important for bed agglomeration.

3.3. Agglomeration mechanisms

The agglomerates formed after controlled agglomeration tests (quartz and olivine) and during operation (K-feldspar) were analyzed to determine what reaction mechanism was responsible for agglomeration. Cross-sections were analyzed to assess what influence the bed material type had on the initial and total defluidization temperatures in Table 2.

Quartz was found to be susceptible to layer-induced agglomeration where alkali from barley straw has likely reacted directly with bed particles to form K-Si-dominated layers based on the extensive interaction with particles, see Fig. 13. This was compounded by adhesion to bed ash particles that form low-viscous melts at higher temperatures. The prevalence of continuous inner layers on bed particles with clear interaction depths into the quartz silicate matrix makes a strictly coating-

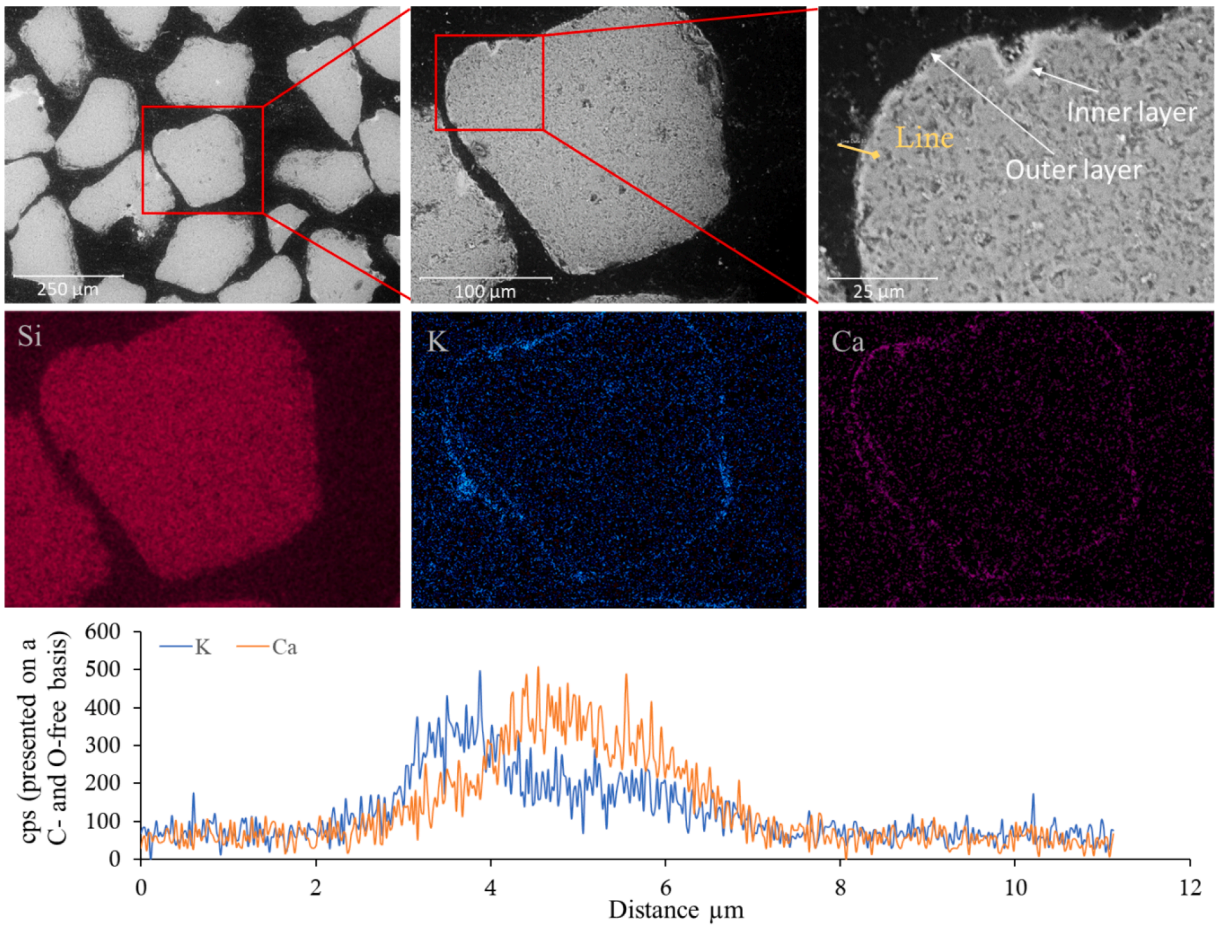

Fig. 8. BSE-SEM micrograph of a typical quartz bed particle after 8 h of barley straw combustion and subsequent agglomeration test. Layers formed due to interaction with bed material are labeled as inner layer or outer layer in accordance with literature. The EDS line analysis clearly shows a K-Ca-rich inner layer, whereas Ca dominates the outer layer over K.

induced interaction pathway unlikely.

In the case of K-feldspar, the agglomeration was at least in part related to the presence of quartz bed particles with extensive alkali interaction. Some interaction with feldspar particles and fuel could be observed, see Fig. 14. The agglomeration mechanism is likely related to molten bed ash, where Ca-adsorption into feldspar particles may increase the severity of these reactions by alkali transport out from the feldspars to layers or bed ash. Further, the layers formed on quartz may also promote agglomeration as they are mainly comprised by K-silicates. This reaction rate seems accelerated, possibly due to the low reactivity of K-feldspar with K-compounds originating from the bed ash.

Agglomerates formed with olivine bed particles and barley straw bed ash were dominated by adhesion to molten bed ash particles (Fig. 15). Only small interactions between bed material and bed ash could be observed where some K or Ca may have reacted with the particles. Therefore, the melting temperature of the bed ash is very important in the case of olivine.

4. Discussion

4.1. Layer formation and agglomeration mechanisms

Barley straw represents a typical agricultural residue with challenging fuel composition with regards to K-silicate melt formation, see Fig. 1. The bed ash interaction with quartz bed particles generally follows proposed layer forming mechanism [6,10,11,33,38], suggesting that alkali compounds from the fuel interact with the bed material under the formation of alkali-rich layers. Furthermore, it has been suggested that these inner layers provide a sticky surface onto which other bed particles or ash particles can stick. The results from this study clearly show that the proposed mechanism is indeed initiated and detected as thin, continuous layers of mainly K on a majority of the bed particles analyzed. Indications of the formation of different layers could also be detected, but to a very small extent.

The layers formed on quartz after agglomeration generally had the same thickness (3–5 µm) as those on the samples from before agglomeration. The mechanisms have been shown to be time and temperature-dependent, and the relatively short experiments (8 h) can explain the lack of significant differences in layer thickness. The increase of K and Ca in the melt can be explained as the result of increased melt formation as both residential time and temperature are increased.

In the case of the agglomerates, thicker layers were identified, suggesting increased reaction rates probably facilitated by proximity to molten bed ash. The composition of ash and melt was found to be very similar in all quartz samples, indicating that the layer formation is dependent on time as well as temperature. This observation matches those reported by He et al. in their studies of time dependency in layer formation on quartz with woody-type fuels [39].

The feldspar showed low tendency for layer formation as the alkali-feldspar particles after agglomeration were scarce, likely affected by the very short operation time possible. This indicates that the bed ash had low interaction with the K-feldspar particles, which has also been reported earlier [36]. Instead, layer formation was observed for quartz bed particles present as contaminations in the bed material. The layer formation on the quartz particles was very similar to that described above (Fig. 7), with continuous thin layers (3 to 5 µm) consisting almost

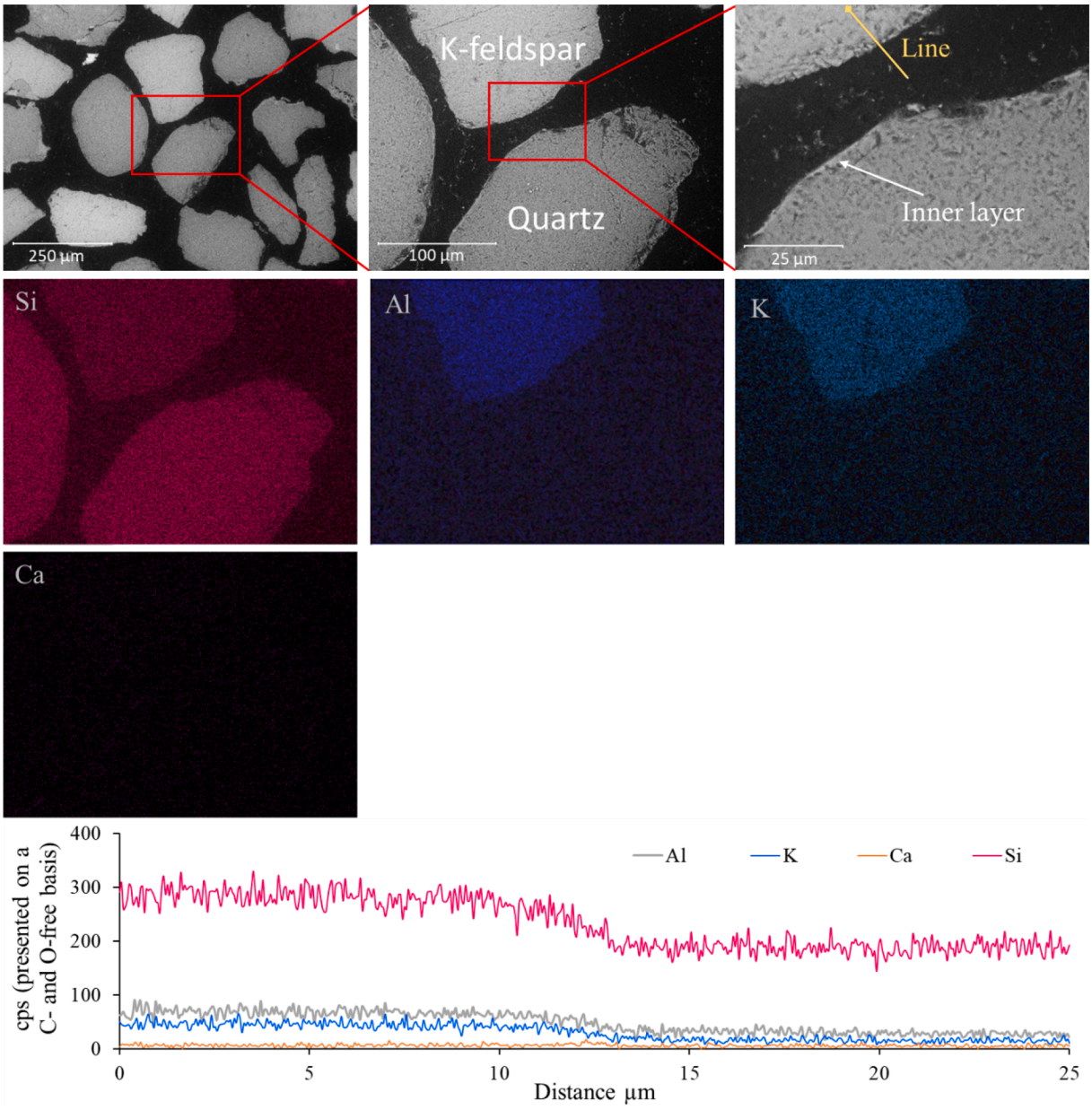

Fig. 9. BSE-SEM micrograph showing typical K-feldspar and quartz bed particles present in natural feldspar after ~ 2 h of barley straw combustion. The inner layer formed on quartz is nearly continuous, but the K-feldspar displayed here had only limited reaction with bed ash, as shown in the EDS line analysis.

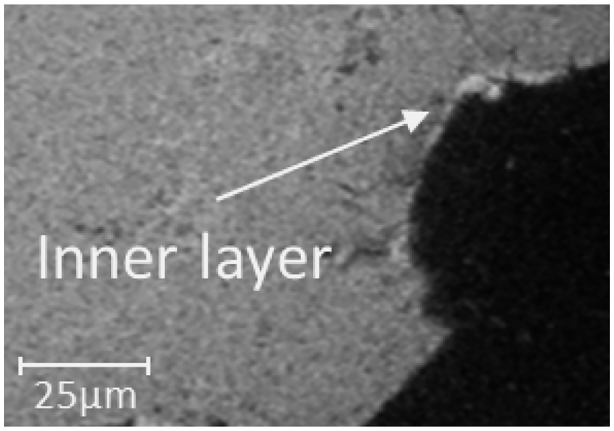

Fig. 10. BSE-SEM micrograph showing typical K-feldspar with a thin Ca-rich inner layer after ~ 2 h of barley straw combustion.

exclusively of K and Ca. However, the agglomerates formed in the feldspar bed showed that the neck's composition varied according to the adjacent particles (Fig. 14).

A proposed mechanism for this behavior is diffusion of K and Na out of K-feldspar and Na-feldspar, respectively, into the necks as the feldspar particles react with Ca. An increase of Na was observed in cases where Na-feldspar was incorporated in the agglomerates. Since K and Na can be expected to have similar properties [4,40], it can be assumed that also K would diffuse into bed ash if the composition favors it [15,18,41]. This diffusion of alkali out of feldspar particles potentially increases the amount of alkali in the bed compared to both the quartz and olivine cases. This is further supported by the low agglomeration temperature in the feldspar experiment. The diffused alkali from the feldspar particles has more opportunities to react further with quartz present as a contaminant in non-pure feldspar and bed ash, as indicated by the SEM-EDS analysis (Fig. 9), indicating that pure K-feldspar would probably have behaved differently regarding the overall performance. These results underline the importance of knowing the bed material's composition and purity to predict and avoid agglomeration problems.

In the olivine cases, both before and after agglomeration, only a few bed particles with formed layers were observed. Those identified were thin (3–5 µm) and discontinuous. This indicates that olivine is less susceptible to alkali-induced layer formation than quartz, as previously suggested [7,14,25]. On the other hand, the significant increase of Mg in the ash and melt of all samples points out that a substitution reaction between Ca, introduced with the fuel, and Mg in the bed particles is taking place, or possibly, Mg migrates from the bed material to the melt.

4.2. Reaction pathways for bed ash and silicate bed material interaction

A general model for silicate bed material reaction with barley straw bed ash is proposed in Fig. 16. The results for barley straw can likely be extended to other agricultural residues due to a common distribution of main ash-forming elements, where the prevalence of K is of particular importance. The general sensitivity of the silicate-based bed materials to extensive and potentially problematic interaction of K-rich bed ash from agricultural residues with bed particles is likely related to the polymerization of silicates. Quartz has a high degree of polymerization and is therefore susceptible to direct attack by alkali compounds through addition reactions, which may be followed by further de-polymerization by Ca-inclusion. Even though the latter may stabilize the layers surrounding a quartz bed particle to reduce its tendency to form agglomerates, it also causes depletion of Ca in the bed ash, which may then increase the risk of agglomeration in prolonged operation.

Feldspars, here represented as $(K,Na)AlSi_3O_8$, differ from quartz in that their possible interactions with bed ash are predominately governed by substitution reactions and are, therefore, not as sensitive to the initial attack by alkali compounds as quartz. For non-feldspar bed particles, this means that higher reaction rates with alkali may be observed since the feldspars do not contribute to alkali sorption. As shown by Hannl et al. [17], Na-feldspars may be susceptible to substitution reactions with K-compounds in the biomass ash, but this leads to a net zero alkali load to the bed ash or non-feldspar bed particles. However, substitution of K^+ or Na^+ in the feldspar with Ca^{2+} causes a net load of alkali transport from bed material to bed ash where each Ca^{2+} potentially causes a release of two alkali cations, either in a gaseous compound such as KOH (g) or to a silicate. The two K^+ released in this substitution may either react with other bed material particles like quartz and thereby initiate layer formation; they could react with the bed ash and thereby push the overall composition towards a lower melting point or be released to the gas phase. This alkali transport mechanism, which has not been previously reported, may pose challenges for bed ash compositions, like those from agricultural residues that will act as a receiving matrix. The presence of a receiving matrix plays a crucial role in this mechanism, which is the transport of alkali from the feldspar to the bed ash. In the case of woody-type biomass or phosphorus-rich residues, K-feldspar has been shown to perform well both under gasification or combustion conditions despite these reactions [5,15-18,41,42]. This is probably due to an already favorable overall fuel ash composition with lower risk of melt formation, as woody-type fuels generally have higher Ca concentrations.

Olivine is completely depolymerized with only SiO_4^{4-} as the silicate part of the matrix. This bed material predominantly reacts by substitution reactions with Ca^{2+} for woody-type biomass, but this also causes a net flow of Mg^{2+} out from the bed particle to bed ash. This is likely, therefore, less detrimental for overall bed ash compositions than the case is for feldspars, where there is a net alkali gain for bed ashes or neighboring bed particles. This was also observed in Fig. 11, where bed ash is deposited as an outer layer rather than the extensive layer formation observed for quartz. Some initial formation of K-Mg-silicates as proposed by Li et al., may be present, and the underlying mechanism here should be investigated further [43]. If this occurs, however, it would suggest a net alkali depletion of bed ash without compromising bed integrity at temperatures prevalent in bubbling fluidized bed combustion of biomass.

4.3. Practical implications

The importance of selecting appropriate bed material for fluidized bed combustion of fuels rich in K is emphasized in this work. Both feldspar and olivine demonstrated limited interactions with the fuel ash. Nevertheless, alkali diffusion out of K/Na-feldspar particles may potentially elevate the alkali content in the bed, suggesting careful consideration for which fuel types feldspar should be used as a bed material. If the potential alkali enrichment in bed ash, as observed here during the combustion of K-rich fuels, interacts with a silicate-dominated bed ash with low Ca content, there is an increased risk of bed agglomeration.

The results suggest that olivine may be the preferable choice among the tested bed materials for prolonged operations for K-rich fuels. However, prolonged exposure to elevated temperatures and alkali metals can also lead to degradation of quartz and olivine particles [43]. Provided sufficient time of operation, the use of quartz as a bed material in fluidized bed combustion increases the risk of agglomeration, as alkali metals in the fuel ash react with the quartz particles, forming low-melting alkali-silicate layers on the quartz particles [6,10,33]. The presence of these adhesive layers on the quartz particles serves as binders, promoting the agglomeration of quartz particles [8,10]. In the case of olivine, the Mg-Ca substitution reaction may impact the mechanical properties and reactivity of the olivine used. This substitution induces a change in the crystal structure, where the larger Ca^{2+} cations, compared to Mg^{2+} ions, can distort the crystal lattice, leading to a

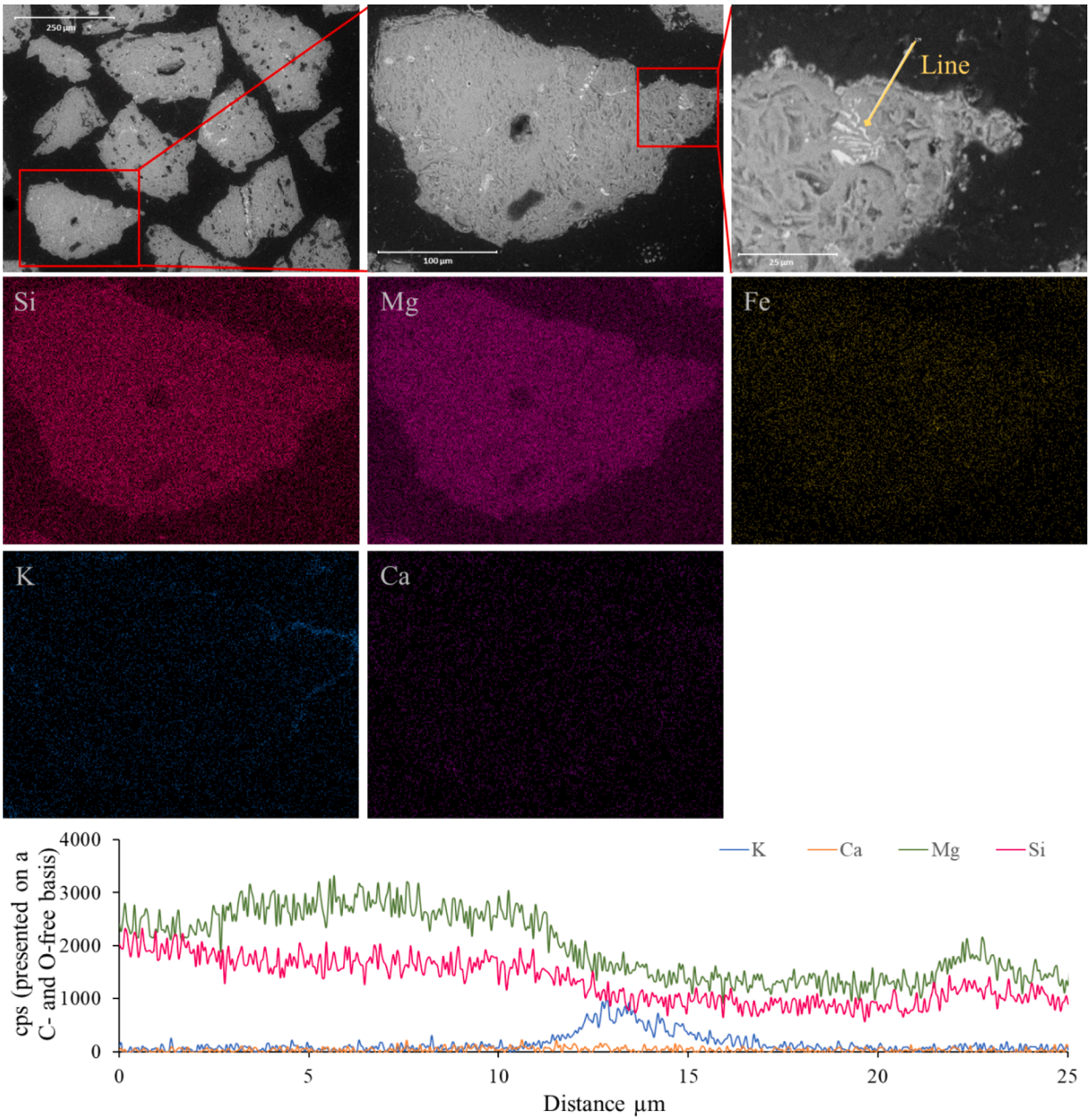

Fig. 11. BSE-SEM micrograph of a typical olivine bed particle after 8 h of barley straw combustion. Outer layers have formed as ash deposition with limited interaction with the bed material itself. The EDS line analysis shows that the non-continuous outer layer is K-rich.

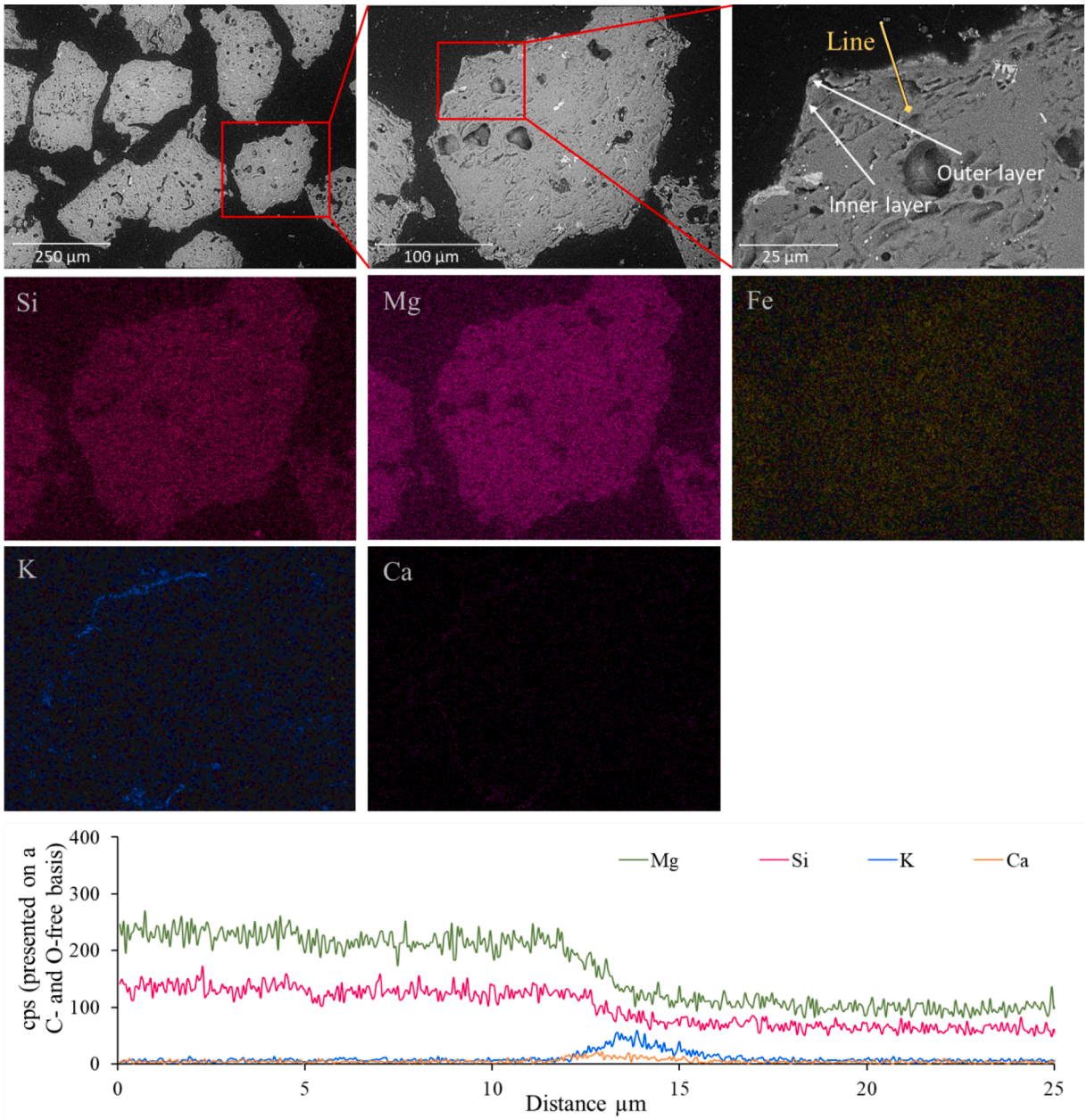

Fig. 12. BSE-SEM micrograph of a typical olivine bed particle after 8 h of barley straw combustion and subsequent agglomeration test. The layer thickness is very small, and the layers are non-continuous, although some interaction has occurred between olivine and the bed ash as indicated by an inner layer. The EDS line analysis shows that the thin layers contain both K and Ca, where Ca is present at higher concentrations than in the sample collected prior to the agglomeration test.

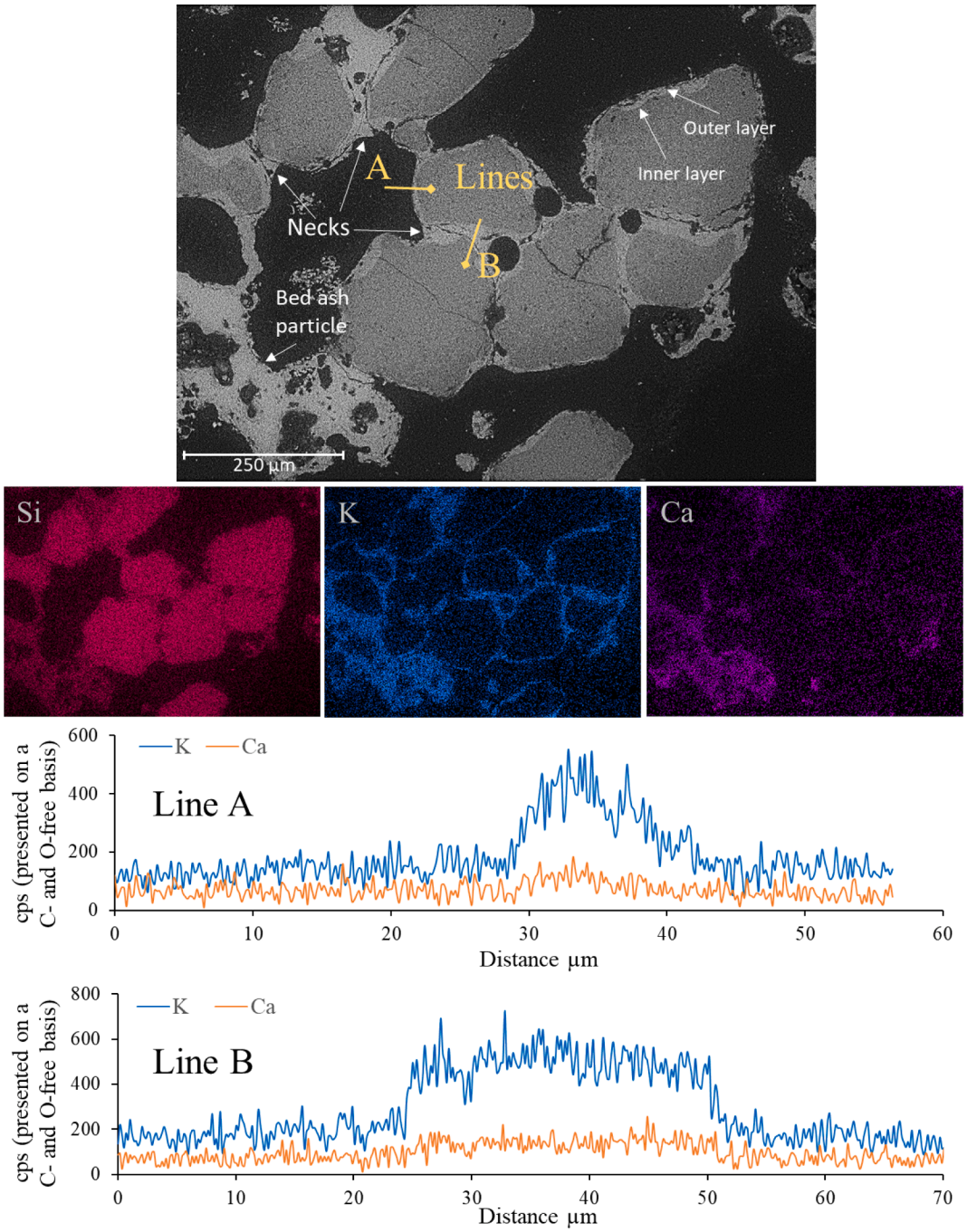

Fig. 13. BSE-SEM micrograph of a typical agglomerate with quartz bed particles after 8 h of barley straw combustion. The K-Si-dominated layers (EDS line analysis A) have similar composition as necks between bed particles (EDS line analysis B). The agglomeration mechanism is likely related to direct attack of alkali on bed particles to form K-Si-rich layers that may bond directly with bed particles or adhere to sticky bed ash particles, as shown in the image.

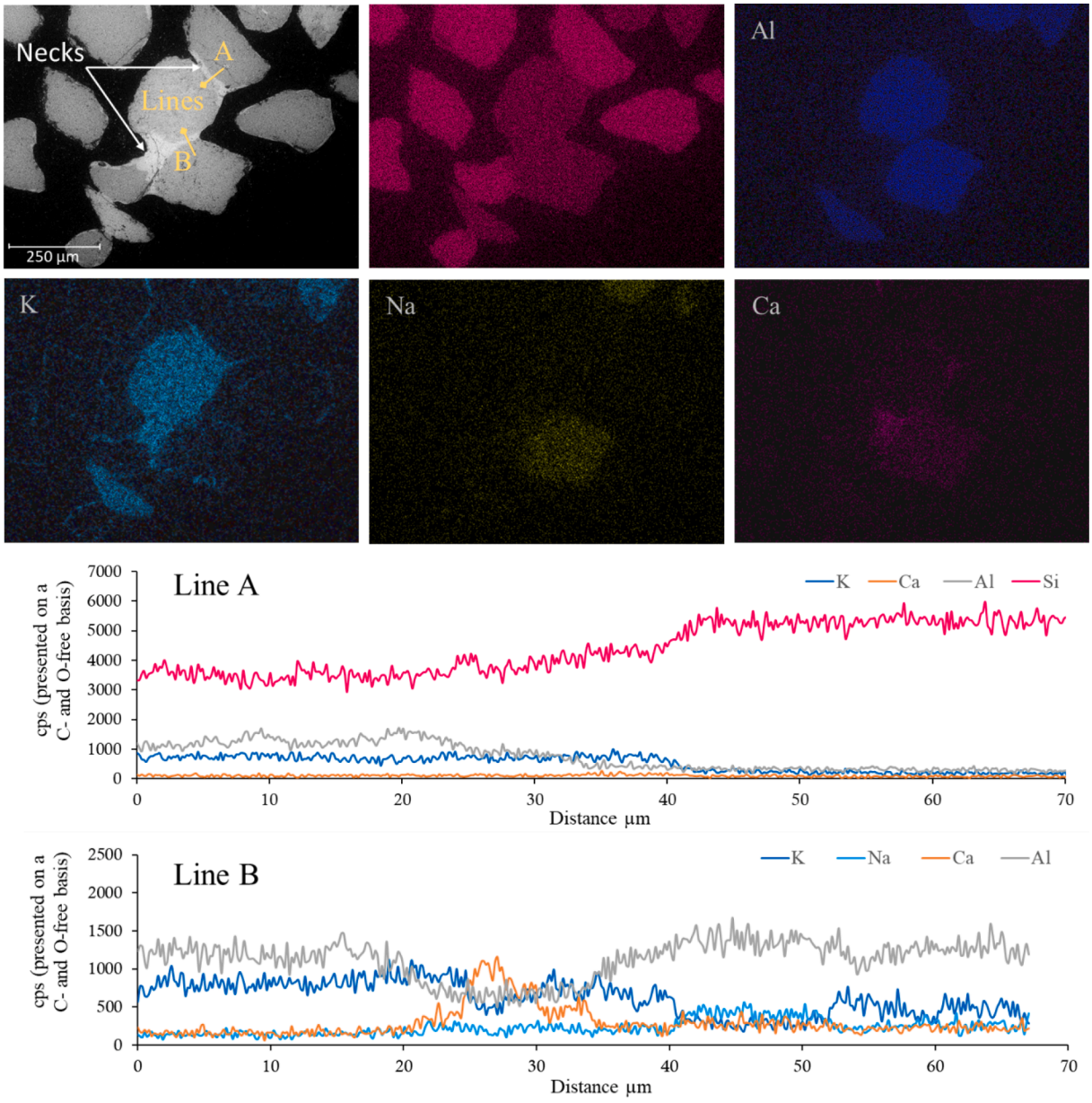

Fig. 14. BSE-SEM micrograph of a typical agglomerate with K-feldspar, Na-feldspar, and quartz bed particles after ~ 2 h of barley straw combustion. The K-Si-dominated neck (EDS line analysis A) between K-feldspar and quartz is K-Si-dominated, and it appears as if there was a low-viscous layer on quartz bonding to the K-feldspar particle. EDS line analysis B shows a neck where bed ash is adhering to K- and -Na-feldspar particles, and Na has seemingly been transported into the neck.

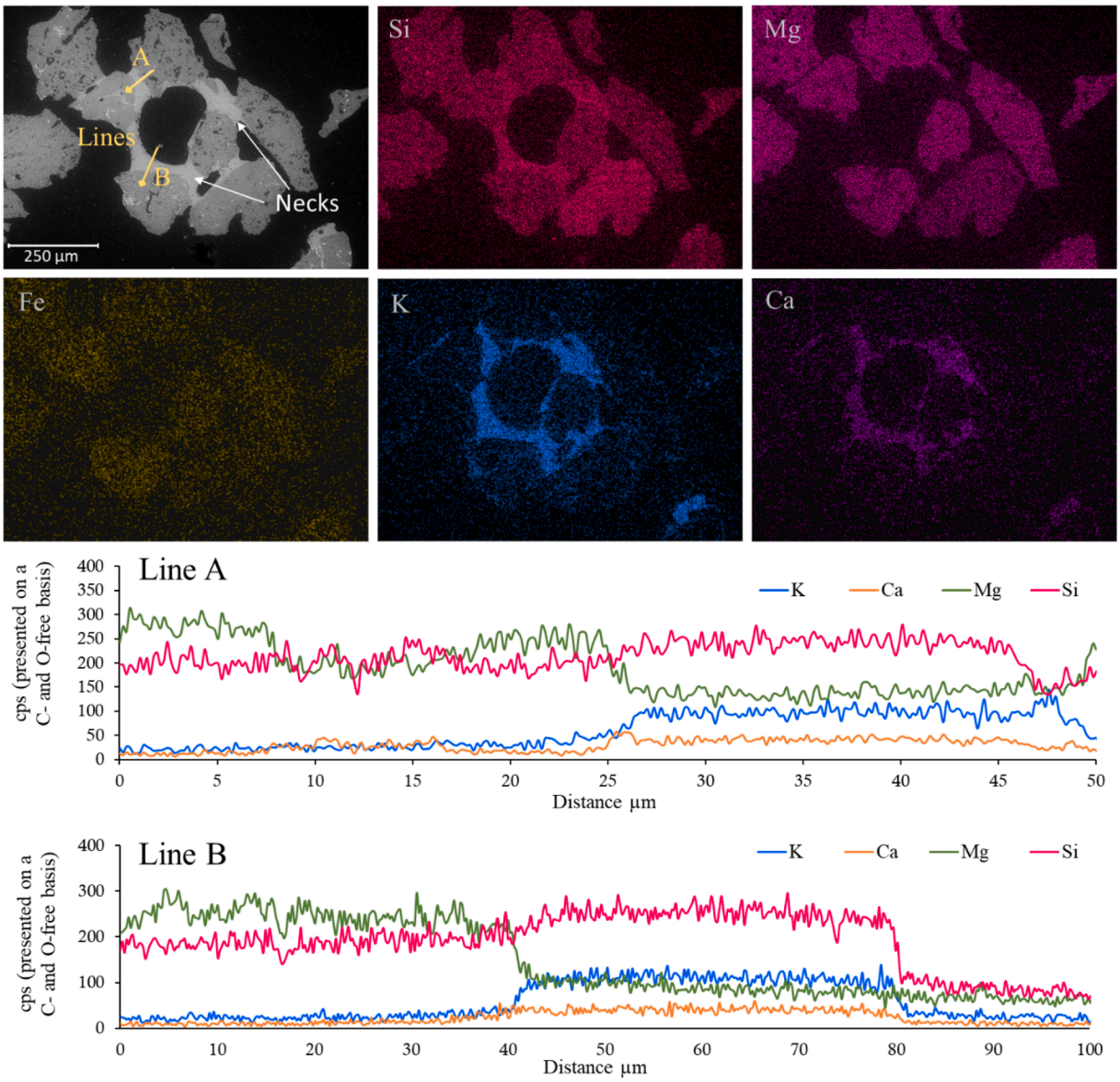

Fig. 15. BSE-SEM micrograph of a typical agglomerate with olivine bed particles after 8 h of barley straw combustion followed by agglomeration test. The K-Si-dominated necks shown in the EDS map create outlines of bed particles rich in Mg, clearly displaying the very low interaction of bed particles and bed ash inside the bed particles. EDS line analysis A suggests that some Mg may be released from the bed material into molten bed ash, but the agglomeration mechanism is governed by the melting points of the bed ash. Similar observations could be made for EDS line analysis B, where it is noticed that Ca maintains a higher concentration in the bed particle than K, suggesting that Ca is preferentially included into the olivine silicate matrix.

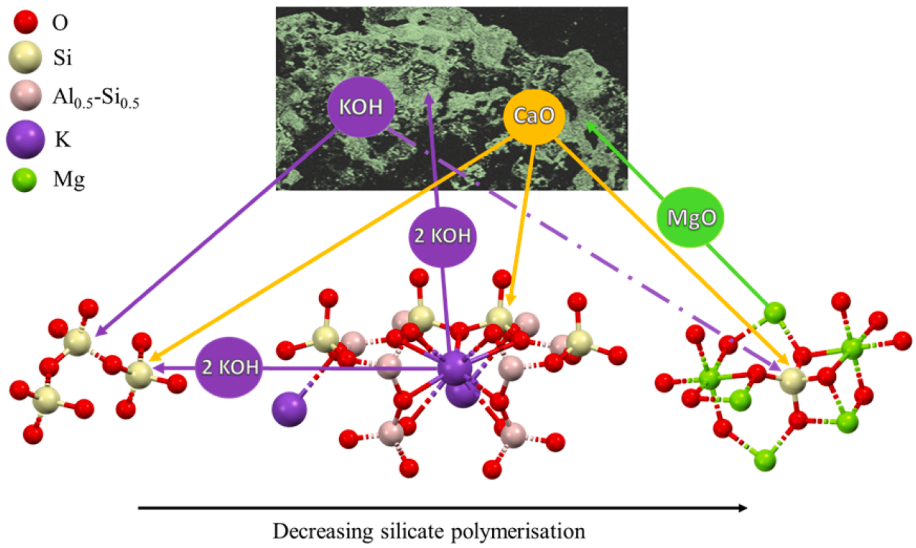

Fig. 16. General model for the reaction between bed ash and the three bed materials investigated in the present work, with ash forming elements represented as oxides or hydroxides. The figure illustrates the degree of polymerization – number of bridging oxygen atoms of the Si-O bonds in the structural framework of quartz, feldspar, and olivine. Quartz exclusively has bridging oxygens, while feldspar exhibits a more complex structure with both bridging and terminal oxygens capable of carrying a charge. Olivine, in contrast, has only terminal oxygens capable of carrying charge. The presence or absence of bridging oxygens influences the properties and behavior of these minerals. Quartz with its high degree of polymerization will undergo an addition reaction (with available cations from the fuel ash) for the quartz particle to carry a charge for further reaction, whereas feldspar and olivine that already carry a charge will undergo substitution reactions with available cations from the fuel ash.

reduction in mechanical strength, as evident from crack formation on olivine bed particles [5,7]. This alternation in the crystal structure may lead to the fractionation of olivine particles, affecting their size. With increased surface area, smaller olivine particles become more susceptible to reacting with fuel ash, thereby elevating the risk of agglomeration during prolonged operations.

5. Conclusions

Barley straw was used as model agriculture residue to investigate the reactivity of three silicate-based bed materials with varying degrees of silicate polymerization with bed ash in bubbling fluidized bed combustion. Under the tested conditions, it was found that:

- Natural K-feldspar performed worse than quartz and olivine, attributed to high degree of alkali reaction with quartz present in the natural feldspar, coupled with simultaneous release of alkali from feldspar for further reactions both with fuel ash and with quartz bed grains.
- Olivine displayed the least interaction with ash-forming elements in the fuel and had the highest initial defluidization temperature of 815 °C where the mechanism responsible for agglomeration was found to be related to the bed ash melting temperature.
- General reaction pathways for reaction of K and Ca in bed ash from agricultural residues with bed material were proposed for the bed materials tested, where the double negative impact for the natural K-feldspar is attributed to Ca depletion in bed ash and active addition to bed ash or quartz from K-feldspar particles. This considers the total elemental transport, both between bed ash and bed material, as well as inter-particle transport in bed material. These transport mechanisms are crucial for successful operation of fluidized beds with agricultural residues as part of an increased bioenergy share in the future global energy supply.

The results emphasize the importance of selecting the correct bed material for the application and fuel intended, as well as the quality, in terms of purity, of the bed material.

CRediT authorship contribution statement

Marjan Bozaghian Bäckman: Conceptualization, Methodology, Formal analysis, Investigation, Resources, Writing – original draft, Writing – review & editing, Visualization, Project administration. **Anders Rebbling:** Conceptualization, Methodology, Formal analysis, Investigation, Writing – original draft, Writing – review & editing, Visualization. **Matthias Kuba:** Writing – review & editing. **Sylvia H. Larsson:** Resources, Writing – review & editing, Funding acquisition. **Nils Skoglund:** Conceptualization, Methodology, Formal analysis, Investigation, Resources, Writing – review & editing, Supervision, Funding acquisition.

Declaration of Competing Interest

The authors declare that they have no known competing financial interests or personal relationships that could have appeared to influence the work reported in this paper.

Data availability

Data will be made available on request.

Acknowledgements

The authors gratefully acknowledge financial support from the Strategic Research Environment Bio4Energy supported through the Swedish Government's Strategic Research Area initiative, Swedish Energy Agency under grant no. 46533-1, and the analytical support (Dr Cheng Choo Lee) from Umeå Core Facility for Electron Microscopy (UCEM) funded by the Swedish Research Council under grant 2019-00217.

Appendix A. Supplementary data

Supplementary data to this article can be found online at https://doi.org/10.1016/j.fuel.2023.130788.

References

[1] IPCC. Climate Change 2022: Mitigation of Climate Change. Contribution of Working Group III to the Sixth Assessment Report of the Intergovernmental Panel on Climate Change. (Intergovernmental Panel on Climate Change, 2022).
[2] IEA. Net Zero by 2050 A Roadmap for the Global Energy Sector. 4th revision ed.: International Energy Agency; 2021:224.
[3] Boström D, Skoglund N, Grimm A, Boman C, Öhman M, Broström M, et al. Ash Transformation Chemistry during Combustion of Biomass. Energy Fuel 2012;26(1):85–93.
[4] Vassilev SV, Vassileva CG, Song YC, Li WY, Feng J. Ash contents and ash-forming elements of biomass and their significance for solid biofuel combustion. Fuel 2017;208:377–409.
[5] Kuba M, Skoglund N, Öhman M, Hofbauer H. A review on bed material particle layer formation and its positive influence on the performance of thermo-chemical biomass conversion in fluidized beds. Fuel 2021;291:120214.
[6] He H, Ji X, Boström D, Backman R, Öhman M. Mechanism of Quartz Bed Particle Layer Formation in Fluidized Bed Combustion of Wood-Derived Fuels. Energy Fuel 2016;30(3):2227–32.
[7] Kuba M, He H, Kirnbauer F, Skoglund N, Boström D, Öhman M, et al. Mechanism of Layer Formation on Olivine Bed Particles in Industrial-Scale Dual Fluid Bed Gasification of Wood. Energy Fuel 2016;30(9):7410–8.
[8] Grimm A, Skoglund N, Boström D, Öhman M. Bed Agglomeration Characteristics in Fluidized Quartz Bed Combustion of Phosphorus-Rich Biomass Fuels. Energy Fuel 2011;25(3):937–47.
[9] Zevenhoven-Onderwater M, Öhman M, Skrifvars BJ, Backman R, Nordin A, Hupa M. Bed agglomeration characteristics of wood-derived fuels in FBC. Energy Fuel 2006;20(2):818–24.
[10] Brus E, Öhman M, Nordin A. Mechanisms of bed agglomeration during fluidized-bed combustion of biomass fuels. Energy Fuel 2005;19(3):825–32.
[11] Öhman M, Pommer L, Nordin A. Bed agglomeration characteristics and mechanisms during gasification and combustion of biomass fuels. Energy Fuel 2005;19(4):1742–8.
[12] Li G, Nathan GJ, Kuba M, Ashman PJ, Saw WL. Interactions of Olivine and Silica Sand with Potassium- or Silicon-Rich Agricultural Residues under Combustion, Steam Gasification, and CO2 Gasification. Ind Eng Chem Res 2021;60(39):14354–69.
[13] Grimm A, Öhman M, Lindberg T, Fredriksson A, Boström D. Bed Agglomeration Characteristics in Fluidized-Bed Combustion of Biomass Fuels Using Olivine as Bed Material. Energy Fuel 2012;26(7):4550–9.
[14] De Geyter S, Öhman M, Boström D, Eriksson M, Nordin A. Effects of non-quartz minerals in natural bed sand on agglomeration characteristics during fluidized bed combustion of biomass fuels. Energy Fuel 2007;21(5):2663–8.
[15] Wagner K, Häggström G, Skoglund N, Priscak J, Kuba M, Öhman M, et al. Layer formation mechanism of K-feldspar in bubbling fluidized bed combustion of phosphorus-lean and phosphorus-rich residual biomass. Appl Energy 2019;248:545–54.
[16] Faust R, Hannl TK, Vilches TB, Kuba M, Ohman M, Seemann M, et al. Layer Formation on Feldspar Bed Particles during Indirect Gasification of Wood. 1. K-Feldspar. Energy Fuel 2019;33(8):7321–32.
[17] Hannl TK, Faust R, Kuba M, Knutsson P, Vilches TB, Seemann M, et al. Layer Formation on Feldspar Bed Particles during Indirect Gasification of Wood. 2. Na-Feldspar. Energy Fuel 2019;33(8):7333–46.
[18] He H, Skoglund N, Öhman M. Time-dependent layer formation on K-feldspar bed particles during fluidized bed combustion of woody fuels. Energy Fuel 2017;31(11):12848–56.
[19] Kuba M, Fursatz K, Janisch D, Aziaba K, Chlebda D, Lojewska J, et al. Surface characterization of ash-layered olivine from fluidized bed biomass gasification. Biomass Convers Biorefin 2021;11(1):29–38.
[20] Lindström E, Sandström M, Boström D, Öhman M. Slagging characteristics during combustion of cereal grains rich in phosphorus. Energy Fuel 2007;21(2):710–7.
[21] Fryda LE, Panopoulos KD, Kakaras E. Agglomeration in fluidised bed gasification of biomass. Powder Technol 2008;181(3):307–20.
[22] Öhman M, Nordin A. The role of kaolin in prevention of bed agglomeration during fluidized bed combustion of biomass fuels. Energy Fuel 2000;14(3):618–24.
[23] Broström M, Kassman H, Helgesson A, Berg M, Andersson C, Backman R, et al. Sulfation of corrosive alkali chlorides by ammonium sulfate in a biomass fired CFB boiler. Fuel Process Technol 2007;88(11–12):1171–7.
[24] Davidsson K, Steenari B-M, Eskilsson D. Kaolin addition during biomass combustion in a 35 MW circulating fluidized-bed boiler. Energy Fuel 2007;21(4):1959–66.
[25] Davidsson K, Åmand L-E, Steenari B-M, Elled A-L, Eskilsson D, Leckner B. Countermeasures against alkali-related problems during combustion of biomass in a circulating fluidized bed boiler. Chem Eng Sci 2008;63(21):5314–29.
[26] Aho M. Reduction of chlorine deposition in FB boilers with aluminium-containing additives. Fuel 2001;80(13):1943–51.
[27] Steenari B-M, Lundberg A, Pettersson H, Wilewska-Bien M, Andersson D. Investigation of ash sintering during combustion of agricultural residues and the effect of additives. Energy Fuel 2009;23(11):5655–62.
[28] Öhman M, Boström D, Nordin A, Hedman H. Effect of kaolin and limestone addition on slag formation during combustion of wood fuels. Energy Fuel 2004;18(5):1370–6.
[29] Steenari B-M, Lindqvist O. High-temperature reactions of straw ash and the anti-sintering additives kaolin and dolomite. Biomass Bioenergy 1998;14(1):67–76.
[30] Tobiasen L, Skytte R, Pedersen LS, Pedersen ST, Lindberg MA. Deposit characteristic after injection of additives to a Danish straw-fired suspension boiler. Fuel Process Technol 2007;88(11–12):1108–17.
[31] Bäfver LS, Rönnbäck M, Leckner B, Claesson F, Tullin C. Particle emission from combustion of oat grain and its potential reduction by addition of limestone or kaolin. Fuel Process Technol 2009;90(3):353–9.
[32] Bozaghian M, Rebbling A, Larsson SH, Thyrel M, Xiong S, Skoglund N. Combustion characteristics of straw stored with CaCO3 in bubbling fluidized bed using quartz and olivine as bed materials. Appl Energy 2018;212:1400–8.
[33] Öhman M, Nordin A, Skrifvars BJ, Backman R, Hupa M. Bed agglomeration characteristics during fluidized bed combustion of biomass fuels. Energy Fuel 2000;14(1):169–78.
[34] Kuba M, He HB, Kirnbauer F, Skoglund N, Bostrom D, Ohman M, et al. Mechanism of Layer Formation on Olivine Bed Particles in Industrial-Scale Dual Fluid Bed Gasification of Wood. Energy Fuel 2016;30(9):7410–8.
[35] Kirnbauer F, Hofbauer H. The mechanism of bed material coating in dual fluidized bed biomass steam gasification plants and its impact on plant optimization. Powder Technol 2013;245:94–104.
[36] Kuba M, He H, Kirnbauer F, Skoglund N, Boström D, Öhman M, et al. Thermal Stability of Bed Particle Layers on Naturally Occurring Minerals from Dual Fluid Bed Gasification of Woody Biomass. Energy Fuel 2016;30(10):8277–85.
[37] Öhman M, Nordin A. A new method for quantification of fluidized bed agglomeration tendencies: A sensitivity analysis. Energy Fuel 1998;12(1):90–4.
[38] Gatternig B, Jr K. Investigations on the mechanisms of ash-induced agglomeration in fluidized-bed combustion of biomass. Energy Fuel 2015;29(2):931–41.
[39] He H, Boström D, Öhman M. Time dependence of bed particle layer formation in fluidized quartz bed combustion of wood-derived fuels. Energy Fuel 2014;28(6):3841–8.
[40] Boström D, Skoglund N, Grimm A, Boman C, Öhman M, Broström M, et al. Ash transformation chemistry during combustion of biomass. Energy Fuel 2011;26(1):85–93.
[41] Wagner K, Häggström G, Mauerhofer AM, Kuba M, Skoglund N, Öhman M, et al. Layer formation on K-feldspar in fluidized bed combustion and gasification of bark and chicken manure. Biomass Bioenergy 2019;127:105251.
[42] Wagner K, Kuba M, Häggström G, Skoglund N, Öhman M, Hofbauer H. Influence of Phosphorus on the Layer Formation to K-Feldspar during Fluidized Bed Combustion and Gasification. In: 26th European Biomass Conference and Exhibition 2018, Copenhagen, Denmark, 14 - 17 May, 2018. 2018:486-92.
[43] Li G, Nathan GJ, Kuba M, Skoglund N, Ashman PJ, Saw WL. Agglomeration of olivine with potassium-or silicon-rich agricultural residues under conditions relevant to dual fluidized bed gasification. Energy Fuel 2022;36(23):14253–66.